EARTHQUAKE ENGINEERING AND STRUCTURAL DYNAMICS
Earthquake Engng. Struct. Dyn. **27**, 977–995 (1998)

ELASTICALLY SUPPORTED CANTILEVER BEAM SUBJECTED TO NONSTATIONARY SEISMIC EXCITATION

GONGKANG FU*
Department of Civil and Environmental Engineering, Wayne State University, Detroit, MI 48202, U.S.A.

SUMMARY

The dynamic behaviour of bridge piers under seismic load is studied here in the context of random vibration. The earthquake excitation is modelled as white noise filtered by the Clough–Penzien filter in cascade with modulation accounting for intensity non-stationarity. The bridge pier modelled as an elastically supported cantilever beam with a lumped mass at the top. An analytical solution is presented for the response statistics, which may be used to develop probabilistic seismic response spectra for design. It is found that the first two modes of the pier approach to rigid-body motion when the stiffness of the elastic support decreases. Seismic responses increase with the top mass, resulting in significantly high displacement and shear but negligible moment at the top, and higher shear and moment at the base. Lower stiffness of the elastic support increases the pier top displacement and moment responses, but may increase or reduce shear responses. The probabilistic spectrum of the relative displacement between the bridge superstructure and the pier top may depend on the two systems' relative modal properties. © 1998 John Wiley & Sons, Ltd.

KEY WORDS: nonstationary; elastically supported cantilever; analytical solution

1. INTRODUCTION

Highway bridges are known to be possibly vulnerable to seismic hazard, especially those elevated by piers because of motion amplification. This has been highlighted by damage to them in several recent earthquakes.[1,2] Understanding of the system's dynamics is important to cover relevant failure modes of bridges in design for both new construction and retrofit.

This paper presents a method to study random vibration of bridge piers subjected to seismic excitation. The bridge pier is modelled as an elastically supported vertical cantilever beam with horizontal seismic excitation at its base. The seismic excitation is modelled by white noise filtered by the Clough–Penzien filter[3] in cascade and then modulated exponentially. Its high-pass subfilter includes high-frequency components in bed rock motion, and the low-pass subfilter models effects of soil in the ground motion. The modulation includes non-stationary intensity of the excitation, since it has been well recognized that non-stationarity of the excitation should be accounted for. Note that random vibration under non-stationary excitation has been studied by many researchers.[4–12] This paper contributes to the knowledge in this area by introducing an analytical solution for a system with infinite degrees of freedom.

* Correspondence to: Gongkang Fu, Department of Civil and Environmental Engineering, Wayne State University, Detroit, MI-48202, U.S.A. E-mail: gfu@ce.eng.wayne.edu

CCC 0098–8847/98/090977–19$17·50

Received 24 September 1995
Revised 2 October 1997 and 26 February 1998

2. MODEL AND FORMULATION

The bridge pier is modelled here as an elastically supported vertical cantilever beam with constant cross-section and an additional lumped mass at the free (top) end. Its horizontal displacement $V(x, t)$ at time t and distance x from its base end is formulated to be governed by the following motion equation, with an assumption of viscous damping:

$$m_c V''(x, t) + c_c V'(x, t) + EIV^{\mathrm{IV}}(x, t) = 0, \quad (t \geqslant 0;\ 0 \leqslant x \leqslant L) \tag{1}$$

where the numbers of primes to $V(x, t)$ indicate the orders of partial derivatives with respect to time t, and the Roman superscript denotes that with respect to location x along the length of the beam. m_c and c_c are constants for mass and damping per unit length, and EI is also a constant denoting the flexural stiffness of the beam. The displacement $V(x, t)$ is decomposed into two parts being pseudo-static displacement $V_s(x, t)$ and dynamic displacement $V_d(x, t)$:

$$V(x, t) = V_s(x, t) + V_d(x, t) \tag{2}$$

The pseudo-static-displacement $V_s(x, t)$ is chosen here as $f(t)\,(1 - x/L)$, essentially describing a rigid-body motion due to the ground displacement $f(t)$. Using equation (2) and assuming the damping term $c_c V_s'(x, t)$ being relatively negligible, equation (1) becomes the following governing equation for the dynamic displacement:

$$m_c V_d''(x, t) + c_c V_d'(x, t) + EIV_d^{\mathrm{IV}}(x, t) = -m_c f''(t)(1 - x/L) \tag{3}$$

The associated initial and boundary conditions are identified as follows:

$$V_d(x, 0) = 0; \quad V_d'(x, 0) = 0 \tag{4}$$

$$k_t V_d(0, t) + EIV_d^{\mathrm{III}}(0, t) = 0, \quad k_r V_d^{\mathrm{I}}(0, t) - EIV_d^{\mathrm{II}}(0, t) = 0 \tag{5a}$$

$$EIV_d^{\mathrm{III}}(L, t) - V''(L, t)m_a = 0, \quad EIV_d^{\mathrm{II}}(L, t) + V''^{,\mathrm{I}}(L, t)J_a = 0 \tag{5b}$$

The boundary conditions in equation (5) describe dynamic equilibrium of forces involving deformations and inertia forces. For the base end of the cantilever beam ($x = 0$), equation (5a) represents an elastic support with resistance to both translation and rocking, whose stiffnesses are denoted by constants k_t and k_r, respectively. This inclusion is intended to model effects of the pier foundation. For example, deep pile foundations may be modelled by setting $k_t \to \infty$ and $k_t \to \infty$. For the top end ($x = L$), equation (5b) includes effects of the additional top mass modelling a pier cap or column flares, which are often used in U.S. highway bridges. m_a and J_a in the equation denote its mass and mass moment of inertia, respectively. Note that $m_a = J_a = 0$ is also not uncommon for a pier with uniform cross-section along its length.

$f''(t)$ in equation (3) includes only horizontal acceleration of earthquake strong motion to the system. It is modelled by a non-stationary and non-white random process, described by combination of a deterministic modulation $\rho(t)$ and a stationary process $f_s(t)$:

$$f''(t) = \rho(t) f_s(t) \quad (t \geqslant 0) \tag{6}$$

$\rho(t)$ is given in a general form

$$\rho(t) = \sum_{i=1,N} A_i \exp(B_i t) \quad (t \geqslant 0) \tag{7}$$

where A_i and B_i are real constants, determined based on the interested strong ground motion records. This general form is selected for ease of derivation to be seen below. $f_s(t)$ is assumed to be a white noise process with zero mean and filtered by the Clough–Penzien filter in cascade.[3] Its power spectral density function is given by

$$S_{ff}(\omega) = \frac{\omega_{g1}^4 + (2\zeta_{g1}\omega_{g1}\omega)^2}{(\omega_{g1}^2 - \omega^2)^2 + (2\zeta_{g1}\omega_{g1}\omega)^2} \frac{\omega^4}{(\omega_{g2}^2 - \omega^2)^2 + (2\zeta_{g2}\omega_{g2}\omega)^2} \frac{S_0}{2\pi} \tag{8}$$

where $\zeta_{g1}, \zeta_{g2}, \omega_{g1}$ and ω_{g2} are characteristic damping ratios and frequencies of the respective subfilters in cascade. S_0 is a constant indicating the intensity of white noise. The autocorrelation function of $f_s(t)$, $R_{ff}(\tau)$, can be analytically obtained by performing the Fourier inverse transform of equation (8)[7,8] and it is explicitly given in Appendix I. As shown by equations (6) and (7), only non-stationarity in ground motion intensity is included in this model, although frequency non-stationarity may also be observed in strong motion records.

3. SOLUTION OF MEAN SQUARE RESPONSE

3.1. Modal decoupling

Equation (3) is solved here by separating the two variables x and t and using modal superposition:

$$V_d(x, t) = \sum_{i=1,2,\ldots} \phi_i(x) V_i(t) \tag{9}$$

where $\phi_i(x)$ is the ith mode shape and $V_i(t)$ is the normal co-ordinate for that mode. Using equation (9) and modal orthogonality, equation (3) becomes a series of decoupled equations of modal motion:

$$V_i''(t) + 2\zeta_i\omega_i V_i'(t) + \omega_i^2 V_i(t) = -S_i f''(t) \quad (i = 1, 2, \ldots) \tag{10}$$

where

$$\omega_i^2 = \left[\int_0^L EI\phi_i^{\mathrm{II}2}(x)\,\mathrm{d}x + k_t\phi_i^2(0) + k_r\phi_i^{\mathrm{I}2}(0)\right] \Big/ \left[\int_0^L m_c\phi_i^2(x)\,\mathrm{d}x + m_a\phi_i^2(L) + J_a\phi_i^{\mathrm{I}2}(L)\right] \tag{11}$$

$$\zeta_i = c_c/(2\omega_i m_c) \tag{12}$$

$$S_i = \int_0^L m_c\phi_i(x)(1 - x/L)\,\mathrm{d}x \Big/ \left[\int_0^L m_c\phi_i^2(x)\,\mathrm{d}x + m_a\phi_i^2(L) + J_a\phi_i^{\mathrm{I}2}(L)\right] \tag{13}$$

The mode shapes are given as

$$\phi_i(x) = c_{1,i}\sin(a_i x) + c_{2,i}\cos(a_i x) + c_{3,i}\sinh(a_i x) + c_{4,i}\cosh(a_i x) \tag{14}$$

a_i in equation (14) is the ith solution of a for the following eigenvalue equation

$$\begin{aligned}
&-[1 + r_m r_J (aL)^4][1 + r_r r_t/(aL)^4] \\
&\quad + \cos(aL)\cos(aL)\{[1 - r_r r_t/(aL)^4][1 - r_m r_J (aL)^4] + 2[r_m r_r + r_t r_J]\} \\
&\quad + \cos(aL)\sinh(aL)\{[1 - r_r r_t/(aL)^4][r_m(aL) - r_J(aL)^3] + [1 - r_m r_J(aL)^4][r_r/(aL) - r_t/(aL)^3]\} \\
&\quad + \sin(aL)\cosh(aL)\{-[1 - r_r r_t/(aL)^4][r_m(aL) + r_J(aL)^3] + [1 - r_m r_J(aL)^4][r_r/(aL) + r_t/(aL)^3]\} \\
&\quad + 2\sin(aL)\sinh(aL)[r_m r_t/(aL)^2 - r_r r_J(aL)^2] = 0
\end{aligned} \tag{15}$$

where

$$r_t = k_t L^3/EI \tag{16}$$

$$r_r = k_r L/EI \tag{17}$$

$$r_J = J_a/(m_c L^3) \tag{18}$$

$$r_m = m_a/(m_c L) \tag{19}$$

These are dimensionless stiffness ratios of the foundation to the beam (equation. (16) for translation and equation (17) for rocking), and inertia ratios of the top mass to the beam mass (equation (18) for rotation

motion and equation (19) for horizontal motion). Equation (15) is derived from the following boundary condition according to equation (5) for non-trivial solutions of $c_{1,i}$ to $c_{4,i}$:

$$r_t\phi_i(0)/L^3 + \phi_i^{\mathrm{III}}(0) = 0, \quad r_r\phi_i^{\mathrm{I}}(0)/L - \phi_i^{\mathrm{II}}(0) = 0 \tag{20a}$$

$$EI\phi_i^{\mathrm{III}}(L)/m_c + \omega_i^2 r_m L\phi_i(L) = 0, \quad EI\phi_i^{\mathrm{II}}(L)/m_c - \omega_i^2 r_J L^3\phi_i^{\mathrm{I}}(L) = 0 \tag{20b}$$

Equation (20b) is derived from equation (5b) with an assumption of the damping term being small compared to those due to the inertia and spring forces, and thus neglected.

Equation (20) determines the mode-shape coefficients $c_{1,i}$ through $c_{4,i}$ in equation (14), with one of them being arbitrary and thus set to be 1 for simplicity:

$$c_{1,i} = 1 \tag{21}$$

$$\begin{aligned} c_{2,i} = \{ &- [\sin(a_iL) + r_J(a_iL)^3\cos(a_iL)][1 + r_rr_t/(a_iL)^4] \\ &+ [(\sinh(a_iL) - r_J(a_iL)^3\cosh(a_iL)][1 - r_rr_t/(a_iL)^4] + 2r_r[\cosh(a_iL) - r_J(a_iL)^3\sinh(a_iL)]/(a_iL)\}/ \\ &\{[\cos(a_iL) - r_J(a_iL)^3\sin(a_iL)][1 + r_rr_t/(a_iL)^4] \\ &- [\cosh(a_iL) - r_J(a_iL)^3\sinh(a_iL)][1 - r_rr_t/(a_iL)^4] + 2r_t[\sinh(a_iL) - r_J(a_iL)^3\cosh(a_iL)]/(a_iL)^3\} \end{aligned} \tag{22}$$

$$c_{3,i} = \{c_{1,i}[1 - r_rr_t/(a_iL)^4] - 2c_{2,i}r_t/(a_iL)^3\}/[1 + r_rr_t(a_iL)^4] \tag{23}$$

$$c_{4,i} = \{2c_{1,i}r_r/(a_iL) + c_{2,i}[1 - r_rr_t/(a_iL)^4]\}/[1 + r_rr_t/(a_iL)^4] \tag{24}$$

3.2. Modal solution in state space

Consider a vector of state variables for mode i:

$$\mathbf{v}_i(t) = (V_i(t), V_i'(t), V_i''(t))^{\mathrm{T}} \tag{25}$$

where superscript T denotes transpose of matrix. Using the impulse response, $\mathbf{v}_i(t)$ can be expressed as the solution to the modal governing equation. Equation (10):[7,11]

$$\mathbf{v}_i(t) = -S_i\mathbf{C}_i\int_0^t \mathbf{z}_i(t-\tau)f''(\tau)\,\mathrm{d}\tau \tag{26}$$

$\mathbf{z}_i(t)$ is the impulse response vector and $\mathbf{C}_i$ is a matrix of system parameters for mode i, respectively:

$$\mathbf{z}_i(t) = (\exp(-\zeta_i\omega_i t)\cos\omega_{di}t, \exp(-\zeta_i\omega_i t)\sin\omega_{di}t, \delta(t))^{\mathrm{T}} \tag{27}$$

$$\mathbf{C}_i = \begin{bmatrix} 0 & 1/\omega_{di} & 0 \\ 1 & -\zeta_i\omega_i/\omega_{\mathrm{d}i} & 0 \\ -2\zeta_i\omega_i & (\zeta_i\omega_i)^2/\omega_{\mathrm{d}i} - \omega_{\mathrm{d}i} & 1 \end{bmatrix} \tag{28}$$

where $\omega_{\mathrm{d}i} = \omega_i(1-\zeta_i^2)^{1/2}$. $\delta(t)$ is the Dirac delta function and satisfies $\int_0^t \delta(t-\tau)f''(\tau)\,\mathrm{d}\tau = f''(t)$. $\mathbf{R}_{\mathbf{v}_i\mathbf{v}_i}(t)$, the covariance matrix of $\mathbf{v}_i(t)$, is then readily formulated as follows, with Ex denoting ensemble expectation:

$$\mathbf{R}_{\mathbf{v}_i\mathbf{v}_i}(t) = Ex[\mathbf{v}_i(t)\mathbf{v}_i^{\mathrm{T}}(t)] = S_i^2\mathbf{C}_i\mathbf{B}_i(t)\mathbf{C}_i^{\mathrm{T}} \tag{29}$$

$$\mathbf{B}_i(t) = \int_0^t\int_0^t \rho(\tau_1)\rho(\tau_2)\mathbf{z}_i(t-\tau_1)R_{ff}(\tau_1-\tau_2)\mathbf{z}_i^{\mathrm{T}}(t-\tau_2)\,\mathrm{d}\tau_1\,\mathrm{d}\tau_2 \tag{30}$$

This double integral has been obtained analytically in the time domain and explicitly given in Reference 7.

It will be seen below that the covariance matrix between two state variable vectors for two different modes (say Modes m and n) is needed for further analysis. This matrix can be similarly expressed as

$$\mathbf{R}_{\mathbf{v}_m\mathbf{v}_n}(t) = Ex[\mathbf{v}_m(t)\mathbf{v}_n^{\mathrm{T}}(t)] = S_mS_n\mathbf{C}_m\mathbf{B}_{mn}(t)\mathbf{C}_n^{\mathrm{T}} \tag{31}$$

$$\mathbf{B}_{mn}(t) = \int_0^t \int_0^t \rho(\tau_1)\rho(\tau_2)\mathbf{z}_m(t-\tau_1)R_{ff}(\tau_1-\tau_2)\mathbf{z}_n^{\mathrm{T}}(t-\tau_2)\,\mathrm{d}\tau_1\,\mathrm{d}\tau_2 \tag{32}$$

The elements of matrix $\mathbf{B}_{mn}(t)$ are explicitly given in Appendix II, and they are derived in the time domain. Note that when $m = n = i$, $\mathbf{B}_{mn}(t) = \mathbf{B}_i(t)$.

3.3. *Mean square responses in state space*

With the elementary terms given above, the covariance matrix $\mathbf{R}_{\mathbf{vv}}(t)$ of the vector of dynamic state variables $\mathbf{v}(t)$ can be now formulated as follows:

$$\begin{aligned}\mathbf{v}(x,t) &= (V_d(x,t),\, V_d'(x,t),\, V_d''(x,t))^{\mathrm{T}} \\ &= \left(\sum_{i=1,2,\ldots}\phi_i(x)V_i(t),\ \sum_{i=1,2,\ldots}\phi_i(x)V_i'(t),\ \sum_{i=1,2,\ldots}\phi_i(x)V_i''(t)\right)^{\mathrm{T}}\end{aligned} \tag{33}$$

$$\begin{aligned}\mathbf{R}_{\mathbf{vv}}(x,t) &= Ex[\mathbf{v}(x,t)\,\mathbf{v}^{\mathrm{T}}(x,t)] = \sum_{m=1,2,\ldots,\ n=1,2,\ldots,}\ \sum \phi_m(x)S_m\phi_n(x)S_n\mathbf{C}_m\mathbf{B}_{mn}(t)\mathbf{C}_n^{\mathrm{T}} \\ &= \begin{bmatrix} R_{vv,11}(x,t) & R_{vv,12}(x,t) & R_{vv,13}(x,t) \\ R_{vv,21}(x,t) & R_{vv,22}(x,t) & R_{vv,23}(x,t) \\ R_{vv,31}(x,t) & R_{vv,32}(x,t) & R_{vv,33}(x,t) \end{bmatrix}\end{aligned} \tag{34}$$

Of the summed terms in equation (34), the dominant terms are often those referring to the same mode, i.e. $(\phi_n(x)S_n)^2\mathbf{C}_n\mathbf{B}_n(t)\mathbf{C}_n^{\mathrm{T}}$ $(n = 1, 2, \ldots)$. With this view, equation (34) describes the total response as summed products of modal response $\mathbf{C}_n\mathbf{B}_n(t)\mathbf{C}_n^{\mathrm{T}}$ and modal participation factor $\phi_n(x)S_n$.

Note that the covariance matrices of other physical quantities can be similarly formulated. For example, the covariance matrices of the state variable vectors for shear force $\mathbf{S}$ and flexural moment $\mathbf{M}$

$$\mathbf{S}(x,t) = EI(V_{\mathrm{d}}^{\mathrm{III}}(x,t),\, V_{\mathrm{d}}^{\mathrm{III}.\prime}(x,t),\, V_{\mathrm{d}}^{\mathrm{III}.\prime\prime}(x,t))^{\mathrm{T}} \tag{35}$$

$$\mathbf{M}(x,t) = EI(V_{\mathrm{d}}^{\mathrm{II}}(x,t),\, V_{\mathrm{d}}^{\mathrm{II}.\prime}(x,t),\, V_{\mathrm{d}}^{\mathrm{II}.\prime\prime}(x,t))^{\mathrm{T}} \tag{36}$$

can be, respectively, expressed as

$$\begin{aligned}\mathbf{R}_{SS}(x,t) &= Ex[\mathbf{S}(x,t)\,\mathbf{S}^{\mathrm{T}}(x,t)] = (EI)^2 \sum_{m=1,2,\ldots,\ n=1,2,\ldots,}\ \sum \phi_m^{\mathrm{III}}(x)S_m\phi_n^{\mathrm{III}}(x)S_n\mathbf{C}_m\mathbf{B}_{mn}(t)\mathbf{C}_n^{\mathrm{T}} \\ &= \begin{bmatrix} R_{SS,11}(x,t) & R_{SS,12}(x,t) & R_{SS,13}(x,t) \\ R_{SS,21}(x,t) & R_{SS,22}(x,t) & R_{SS,23}(x,t) \\ R_{SS,31}(x,t) & R_{SS,32}(x,t) & R_{SS,33}(x,t) \end{bmatrix}\end{aligned} \tag{37}$$

$$\begin{aligned}\mathbf{R}_{\mathbf{MM}}(x,t) &= Ex[\mathbf{M}(x,t)\,\mathbf{M}^{\mathrm{T}}(x,t)] = (EI)^2 \sum_{m=1,2,\ldots,\ n=1,2,\ldots,}\ \sum \phi_m^{\mathrm{II}}(x)S_m\phi_n^{\mathrm{II}}(x)S_n\mathbf{C}_m\mathbf{B}_{mn}(t)\mathbf{C}_n^{\mathrm{T}} \\ &= \begin{bmatrix} R_{MM,11}(x,t) & R_{MM,12}(x,t) & R_{MM,13}(x,t) \\ R_{MM,21}(x,t) & R_{MM,22}(x,t) & R_{MM,23}(x,t) \\ R_{MM,31}(x,t) & R_{MM,32}(x,t) & R_{MM,33}(x,t) \end{bmatrix}\end{aligned} \tag{38}$$

4. NUMERICAL EXAMPLES

For a typical reinforced concrete pier of highway bridges in U.S., the following parameters were selected: $L = 8$ m, $EI/m_c = 214{\cdot}3$ kN/kg m^3, and $\zeta_i = 0{\cdot}04$ $(i = 1, 2, \ldots)$. This constant damping ratio was used because it was felt that the one inversely proportional to the modal frequency as defined in equation (12) is

Table I. Dimensionless eigenvalue a_iL for numerical examples

i	Case I-1 $r_t = r_r = \infty$, $r_m = r_J = 0$	Case I-2 $r_t = r_r = \infty$, $r_m = 0{\cdot}2$, $r_J = 0{\cdot}0004$	Case I-3 $r_t = r_r = \infty$, $r_m = 0{\cdot}4$, $r_J = 0{\cdot}0008$
1	1·875	1·616	1·471
2	4·694	4·242	4·103
3	7·8548	7·2012	7·0135
4	10·99554	10·06044	9·70237
i	Case II-1 $r_t = 10$, $r_r = 1$, $r_m = r_J = 0$	Case II-2 $r_t = 10$, $r_r = 1$, $r_m = 0{\cdot}2$, $r_J = 0{\cdot}0004$	Case II-3 $r_t = 10$, $r_r = 1$, $r_m = 0{\cdot}4$, $r_J = 0{\cdot}0008$
1	1·196	1·067	0·987
2	2·505	2·383	2·334
3	4·9751	4·5385	4·4086
4	7·98395	7·33470	7·14670
i	Case III-1 $r_t = 1$, $r_r = 0{\cdot}1$, $r_m = r_J = 0$	Case III-2 $r_t = 1$, $r_r = 0{\cdot}1$, $r_m = 0{\cdot}2$, $r_J = 0{\cdot}0004$	Case III-3 $r_t = 1$, $r_r = 0{\cdot}1$, $r_m = 0{\cdot}4$, $r_J = 0{\cdot}0008$
1	0·698	0·628	0·582
2	1·482	1·419	1·393
3	4·7593	4·3016	4·1599
4	7·86783	7·21505	7·02735

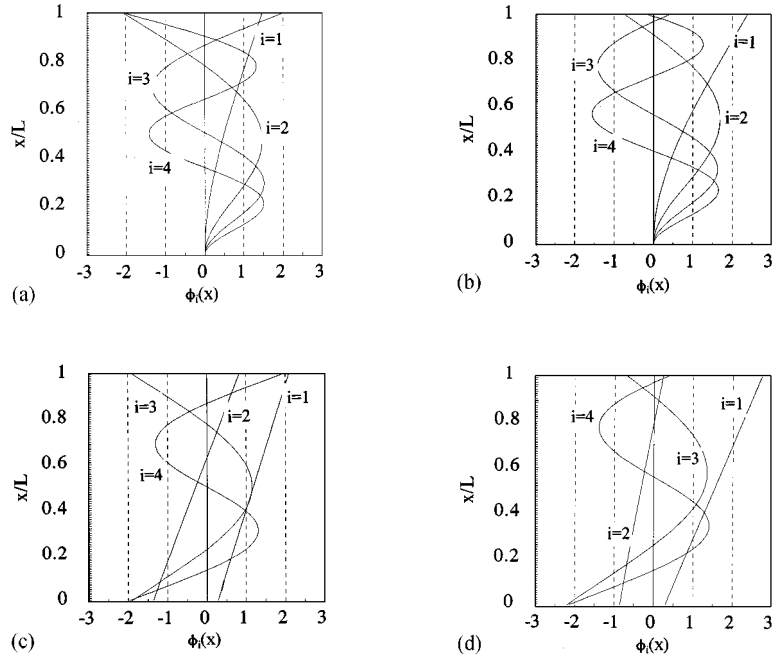

Figure 1. First 4 mode shapes: (a) Case I-1; (b) Case I-3; (c) Case III-1; (d) Case III-3

not realistic for concrete structures. Several typical sets of stiffness ratios r_t and r_r and inertia ratios r_J and r_m were selected to be studied here. They represent deep pile foundations with $k_t \to \infty$ and $k_r \to \infty$ or spread footings with smaller k_t and k_r, and piers with uniform cross section ($J_a = m_a = 0$) or with flares ($J_a > 0$, $m_a > 0$). These cases are listed in Table I with the associated dimensionless eigenvalues used to obtain the natural frequencies. Figure 1 shows the first 4 mode shapes for 4 of these cases. Note that these mode shapes have been normalized, i.e.

$$\int_0^L \phi_i^2(x)\,\mathrm{d}x = 1, \quad (i = 1, \ldots, 4)$$

Comparison of these figures indicates that increasing inertia ratios r_J and r_m result in nodal points of these modes moving up, and decreasing stiffness ratios r_t and r_r lead to these nodal points moving down. Decrease of the foundation stiffness causes the first two modes to approach to rigid-body motion.

For the first 4 modes, Table II shows the modal participation factors $\phi_i(L)S_i$ for the displacement at the top end ($x = L$). These modal participation factors have no dimensions by definition (equations (13) and (14)), and indicate the mode's participation in the total response of top displacement as shown in equation (34). Table II shows that the first mode has relatively higher mode participation factor with increase of r_J and r_m and decrease of r_t and r_r, indicating its more significant contribution.

Shinozuka–Sato modulation[13] was used here in the examples by setting $N = 2$, $A_1 = 12{\cdot}8$, $A_2 = -12{\cdot}8$, $B_1 = -0{\cdot}14$, and $B_2 = -0{\cdot}19$ in equation (7) for the Taft earthquake.[6] This modulation function models non-stationary intensity of earthquakes with moderate intensity building-up, and it reaches the maximum at t approximately equal to 6·1 s. The filter parameters were selected as $\zeta_{g1} = 0{\cdot}65$, $\zeta_{g2} = 0{\cdot}5$, $\omega_{g1} = 6{\cdot}4\pi$ rad/s, and $\omega_{g2} = 0{\cdot}32\pi$ rad/s.[14]

For unit S_0, Figures 2 and 3 show the 6 independent terms of $\mathbf{R}_{vv}(L, t)$, the covariance matrix of top displacement, for 4 of the boundary condition cases. They include 3 diagonal terms $R_{vv,kk}$ ($k = 1, 2, 3$) and 3 correlation coefficients $\gamma_{vv,jk} = R_{vv,jk}/(R_{vv,jj}R_{vv,kk})^{1/2}$ ($j, k = 1, 2, 3$; $j \neq k$). Four modes were found to be adequate for convergence of equation (34) for all the cases studied here. Note that for those cases with higher r_J and r_m, and lower r_t and r_r, fewer modes are required for convergence, because the first mode is more

Table II. Modal participation factor $\phi_i(L)S_i$ for Top Displacement. $V_d(L, t)$

Mode i	Case I-1 $r_t = r_r = \infty$, $r_m = r_J = 0$	Case I-2 $r_t = r_r = \infty$, $r_m = 0{\cdot}2$, $r_J = 0{\cdot}0004$	Case I-3 $r_t = r_r = \infty$, $r_m = 0{\cdot}4$, $r_J = 0{\cdot}0008$
1	0·428	0·234	0·160
2	− 0·686	− 0·328	− 0·212
3	0·444	0·148	0·080
4	− 0·331	− 0·060	− 0·015
	Case II-1	Case II-2	Case II-3
Mode i	$r_t = 10$, $r_r = 1$, $r_m = r_J = 0$	$r_t = 10$, $r_r = 1$, $r_m = 0{\cdot}2$, $r_J = 0{\cdot}0004$	$r_t = 10$, $r_r = 1$, $r_m = 0{\cdot}4$, $r_J = 0{\cdot}0008$
1	0·543	0·340	0·246
2	− 0·618	− 0·386	− 0·278
3	0·088	0·056	0·041
4	− 0·017	− 0·003	− 0·001
	Case III-1	Case III-2	Case III-3
Mode i	$r_t = 1$, $r_r = 0{\cdot}1$, $r_m = r_J = 0$	$r_t = 1$, $r_r = 0{\cdot}1$, $r_m = 0{\cdot}2$, $r_J = 0{\cdot}0004$	$r_t = 1$, $r_r = 0{\cdot}1$, $r_m = 0{\cdot}4$, $r_J = 0{\cdot}0008$
1	0·551	0·356	0·261
2	− 0·560	− 0·361	− 0·265
3	0·011	0·010	0·009
4	− 0·002	− 0·002	− 0·003

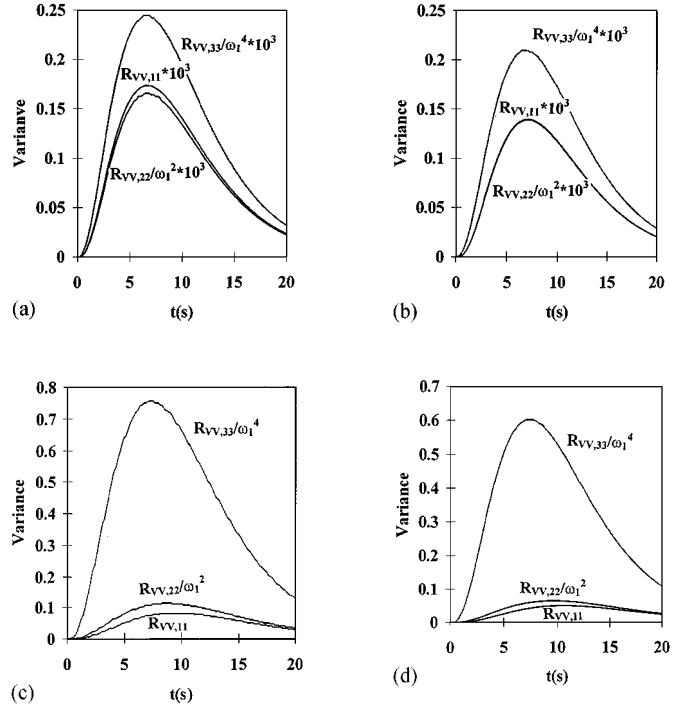

Figure 2. Variances of top displacement, velocity, and acceleration: (a) Case I-1; (b) Case I-3; (c) Case III-1; (d) Case III-3

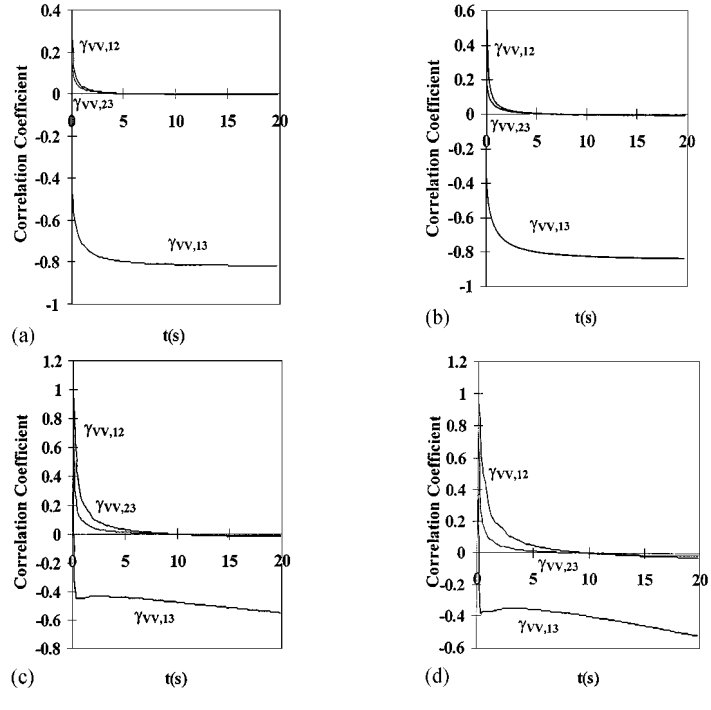

Figure 3. Correlation coefficients between top displacement, velocity, and acceleration: (a) Case I-1; (b) Case I-3; (c) Case III-1; (d) Case III-3

dominant as discussed earlier. The three diagonal terms of equation (34) are the variances of displacement $V_d(L, t)$, velocity $V'_d(L, t)$, and acceleration $V''_d(L, t)$ at the top of the bridge pier. ω_1 is the first natural frequency of the pier system. When the pier is rigidly supported ($r_t = r_r \to \infty$) and without additional mass ($r_J = r_m = 0$) in Case I-1, the peaks of acceleration, velocity, and displacement (variances $R_{vv,33}$, $R_{vv,22}$, and $R_{vv,11}$) occur almost simultaneously at about $t = 6.4$ s, being close to the modulation function's maximum point. With the natural frequencies reduced by increasing top mass in Case I-3, these peaks are slightly delayed. Reduction of the foundation stiffness in Cases III-1 and III-3 delays these peaks much more, apparently due to more significant decrease of the natural frequencies, especially for velocity and displacement (Variances $R_{vv,22}$, and $R_{vv,11}$). Figure 2 also shows, in general, higher response for higher inertia ratios r_J and r_m or lower stiffness ratios r_t and r_r. This is mainly because modes with lower natural frequencies respond more severely for the displacement at the pier top. Figure 3 shows that the correlation coefficients reach relatively stationary levels earlier for Case I-1 with higher natural frequencies and later for the cases with lower natural frequencies, especially for that between displacement and acceleration ($\gamma_{vv,13}$). Note that this correlation coefficient is typically negative.

For the cases of shear and moment to be discussed below, 6 mode were required for convergence of equations (37) and (38). Figure 4 shows the variance of the base shear force $R_{SS,11}(0, t)$ for several cases of boundary condition compared to that for rigid support without additional top mass (Case I-1). Results of comparison between the peak values are also indicated for each case, which are of interest for practical

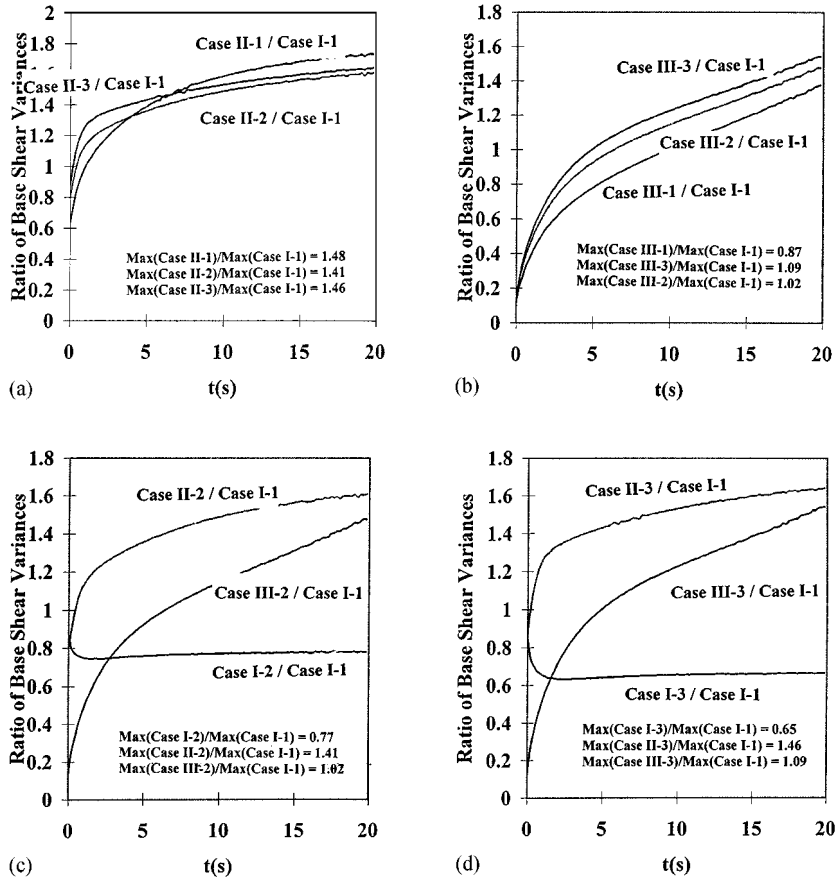

Figure 4. Comparison of base shear force variances: (a) Cases II; (b) Cases III; (c) Cases 2; (d) Cases 3

reasons such as design consideration. Figures 4(a) and 4(b) show that higher top mass increases the peak shear force response. Figures 4(c) and 4(d) show that the peak shear force response initially increases when the foundation stiffness reduces from rigid to $r_t = 10$ and $r_r = 1$. Further reduction to $r_t = 1$ and $r_r = 0{\cdot}1$ does not further increase the response. This perhaps is due to varying contents of natural frequency in each of these cases, which results in various modal participation factors and modal responses. Figure 5 shows the same comparison as in Figure 4 for $R_{MM,11}(0, t)$, the flexural moment at the pier base. The peak moment response reduces with the top mass or the foundation stiffness. Figures 5(a) and 5(b) also show that stiffness ratios $r_t = 1$ and $r_r = 0{\cdot}1$ lead to decrease of the peak moment, and $r_t = 10$ and $r_r = 1$ causes its increase. Table III shows calculation convergence in shear and moment, with respect to the number of modes used. As discussed earlier, 'softer' systems (Cases III-1 and III-3) converge faster.

Figures 6 and 7 display $R_{SS,11}(L, t)$ and $R_{MM,11}(L, t)$, the variances of the shear force and flexural moment at the pier top, compared with those at the pier base for Case I-1. Figures 6(a), 6(b), 7(a) and 7(b) show the same behaviour seen in Figures 4(a), 4(b), 5(a) and 5(b), i.e. the responses increase with the top mass, as intuitively expected. Figures 6(c) and 6(d) exhibit similar behaviour as seen in Figures 4(c) and 4(d), i.e. change of foundation stiffness does not monotonically change the peak response level. On the other hand, Figure 7(c) and 7(d) show the trend of decreasing response with the foundation stiffness. It is worth noting

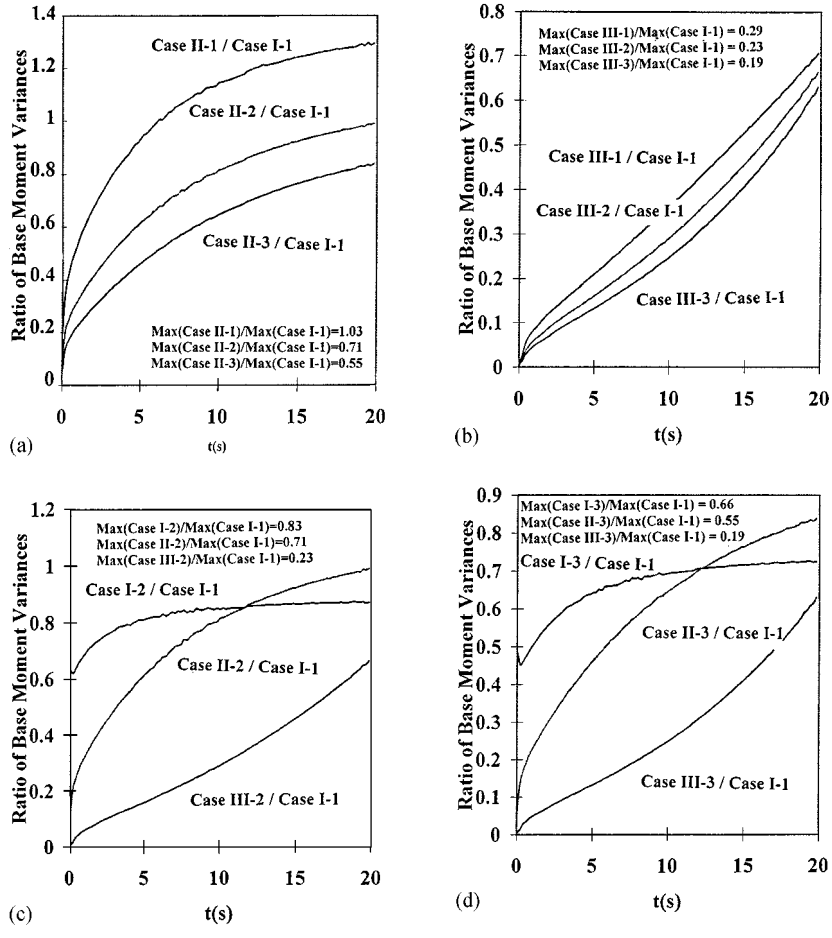

Figure 5. Comparison of base flexural moment variances: (a) Cases II; (b) Cases III; (c) Cases 2; (d) Cases 3

Table III. Convergence behaviour of base shear and base moment

(a) Base shear			Max $R_{SS,11}(0,t)/(\omega_1^2 m_c L^2)^2$		
Number of modes			4	5	6
Case	I-1	$(\times 10^8)$	0·630	0·650	0·665
	I-3	$(\times 10^7)$	0·275	0·290	0·299
	III-1	$(\times 10^4)$	0·157	0·157	0·157
	III-3	$(\times 10^4)$	0·842	0·842	0·842
(a) Base moment			Max $R_{MM,11}(0,t)/(\omega_1^2 m_c L^2)^2$		
Number of modes			4	5	6
Case	I-1	$(\times 10^{10})$	0·235	0·235	0·236
	I-3	$(\times 10^9)$	0·109	0·109	0·109
	III-1	$(\times 10^6)$	0·184	0·184	0·184
	III-3	$(\times 10^6)$	0·530	0·530	0·530

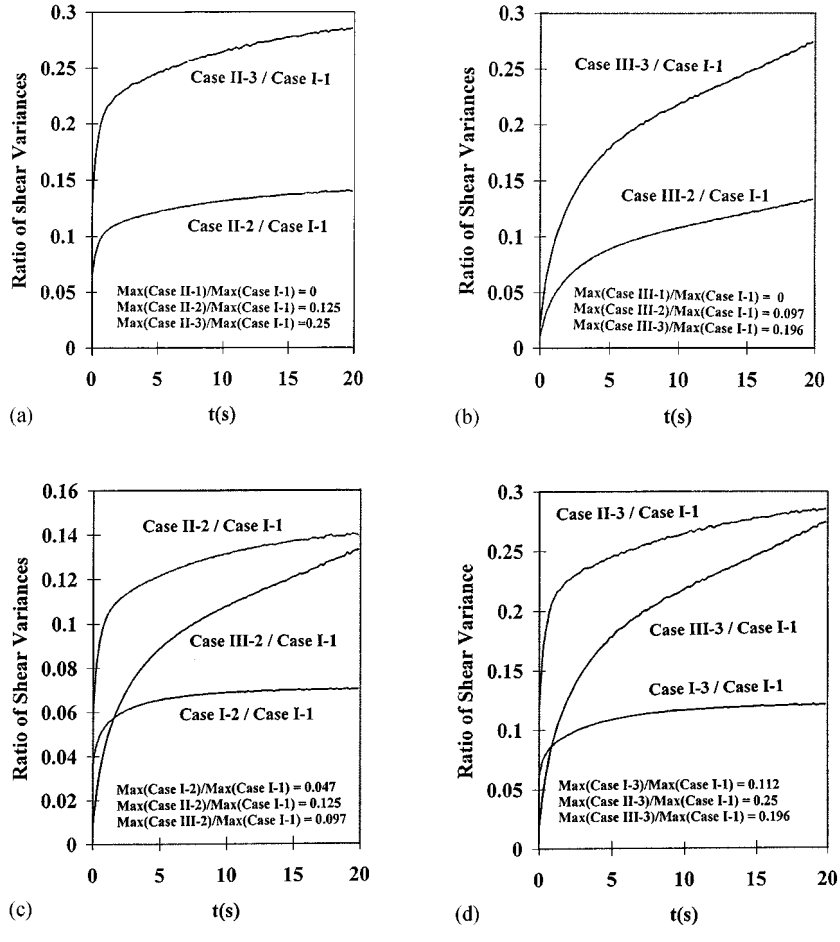

Figure 6. Comparison of shear force variances at top vs. at base: (a) Cases II; (b) Cases III; (c) Cases 2; (d) Cases 3

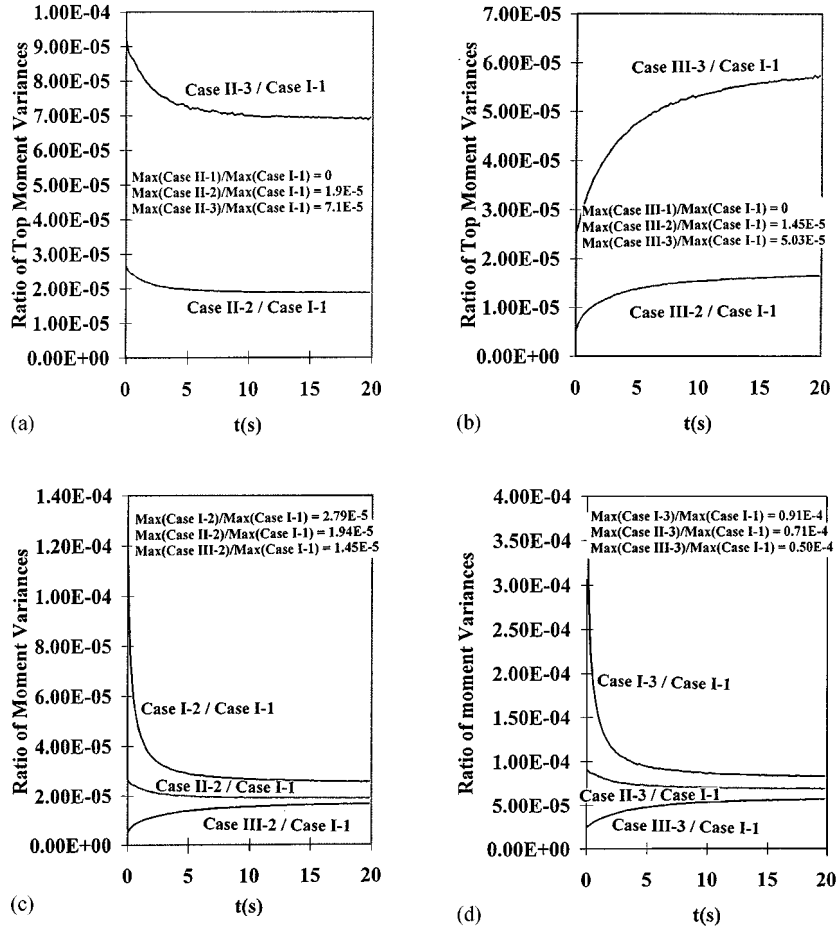

Figure 7. Comparison of flexural moment variances at top vs. at base: (a) Cases II; (b) Cases III; (c) Cases 2; (d) Cases 3

that the peak response of shear force variance at the top could be as high as 25 per cent of the base shear variance in the case of rigid support without top mass (Case II-3 in Figure 6d), simply due to addition of the top mass. This shows how pier caps or column flares may contribute to severe strength requirement for the pier or possibly failure. On the other hand, the moment at the top is shown to be negligible for these typical values of r_J and r_m (Figure 7).

The mean square response statistics shown here may be used to develop probabilistic seismic response spectra for interested failure modes. An example is given here. Consider a bridge span with one end supported by an abutment with fixed bearings and the other by a pier with expansion bearings. The fixed bearings and the bridge deck (superstructure) are modelled as an SDOF system with frequency ω_0 and damping ratio ζ subjected to the strong motion acceleration $f''(t)$ through the abutment:

$$w''(t) + 2\zeta\omega_0 w'(t) + \omega_0^2 w(t) = -f''(t) \tag{39}$$

where $w(t)$ is the horizontal displacement of the deck relative to the abutment. The relative displacement $u(t)$ at the end supported by the pier is focused here:

$$\mathbf{u}(t) = \mathbf{w}(t) - \mathbf{V}(L, t) \tag{40}$$

where $\mathbf{u}(t) = (u(t), u'(t), u''(t))^{\mathrm{T}}$. Understanding the dynamics of this system is critical in considering the failure mode of span collapse due to excessive relative displacement $u(t)$.

The covariance matrix of $\mathbf{u}(t)$ can be expressed as

$$\mathbf{R}_{\mathbf{uu}}(t) = \mathbf{R}_{\mathbf{ww}}(t) - \mathbf{R}_{\mathbf{wV}}(L, t) - \mathbf{R}_{\mathbf{Vw}}(L, t) + \mathbf{R}_{\mathbf{VV}}(L, t) \tag{41}$$

where

$$\mathbf{R}_{\mathbf{wV}}(L, t) = Ex[\mathbf{w}(t)\mathbf{V}^{\mathrm{T}}(L, t)] \tag{42}$$

$$\mathbf{R}_{\mathbf{Vw}}(L, t) = Ex[\mathbf{V}(L, t)\mathbf{w}^{\mathrm{T}}(t)] \tag{43}$$

The detailed expressions of Equations (42) and (43) can be readily derived in a similar manner to equation (34), viewing the motion of $\mathbf{w}(t)$ as that of another mode with frequency ω_0, damping ratio ζ, and a modal participation factor of 1.

Now let $E[M(-\infty, t)]$ be the mean rate of displacement maxima at time t and $E[M(U, t)]$ be the mean rate of displacement maxima above a given level U, they are, respectively,[15]

$$E[M(-\infty, t)] = -\int_{-\infty}^{\infty} \mathrm{d}u \int_{-\infty}^{0} \ddot{u} p_{u,\dot{u},\ddot{u}}(u, 0, \ddot{u}, t)\, \mathrm{d}\ddot{u} \tag{44}$$

$$E[M(U, t)] = -\int_{U}^{\infty} \mathrm{d}u \int_{-\infty}^{0} \ddot{u} p_{u,\dot{u},\ddot{u}}(u, 0, \ddot{u}, t)\, \mathrm{d}\ddot{u} \tag{45}$$

where $p_{u,\dot{u},\ddot{u}}(\cdot)$ is the joint probability density function for $u(t)$, $u'(t)$ and $u''(t)$. If $f''(t)$ is assumed to be a Gaussian excitation, these state variables are also Gaussian variables. $E[M(-\infty, t)]$ and $E[M(U, t)]$ have been explicitly given for this case in Reference 7. Let probability of failure due to excessive displacement be

$$P_f = \text{Probability [maximum } u(t) > U] = \int_0^{T_s} E[M(U, t)]\, \mathrm{d}t \Big/ \int_0^{T_s} E[M(-\infty, t)]\, \mathrm{d}t \tag{46}$$

where T_s is the interested time length, being the time interval of significant seismic input. P_f indicates the likelihood that peak displacements exceed a given level U. Variation of the threshold level U as a function of $T = 2\pi/\omega_0$ and ζ (period and damping ratio of the superstructure system) is defined here as probabilistic displacement response spectrum, because it is associated with a probability to be exceeded. The integrations in equation (46) were performed numerically by the Simpson's rule. Figure 8 demonstrates two examples for $S_0 = 0{\cdot}01\ \mathrm{m}^2/\mathrm{s}^3$, $P_f = 0{\cdot}1$ and $\zeta = 0{\cdot}03$ and $0{\cdot}05$. These curves show that the threshold U generally increases with the period T except in the areas of $T = 0{\cdot}4$, $1{\cdot}8$ and $2{\cdot}6$ s for Cases I-3, III-1, and III-3, respectively. These dips are caused by coincidence between the frequencies ω_0 and ω_1, respectively of the superstructure SDOF system and the pier system. This coincidence results in very much similar motions of the two systems,

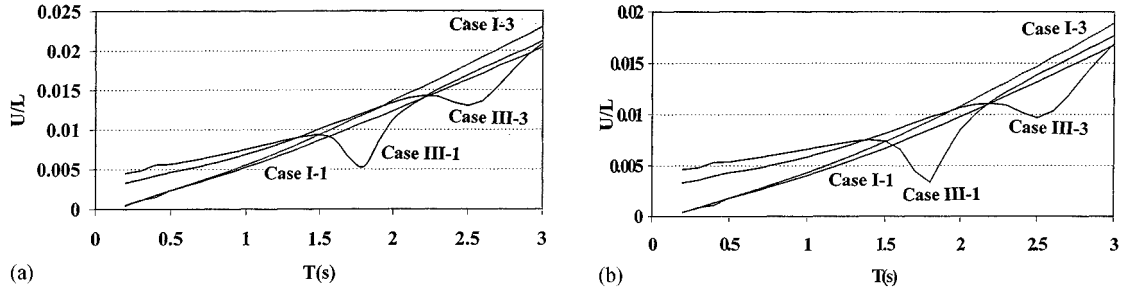

Figure 8. Spectra of relative displacement with probability of 0·1 to be exceeded: (a) $\xi = 0{\cdot}03$; (b) $\xi = 0{\cdot}05$

which in turn leads to much lower relative response of $\mathbf{R}_{uu}(t)$ in equation (41), particularly when the first mode dominantly contributes to the pier's total response. When this occurs, it is equivalent to state that the two systems' responses are much correlated. These spectra may be used for design of controlling the relative displacement to cover the span-falling failure mode.

5. CONCLUSIONS

An explicit solution is presented in this paper for random vibration of an elastically supported cantilever beam subjected to modulated filtered excitation, including a general form of modulation. This solution may be used to develop probabilistic seismic response spectra for seismic bridge design in addressing the failure mode of excessive relative displacement. It is also shown that the first two modes approach to rigid-body motion when the stiffness of the pier foundation decreases. The top mass may cause significantly high displacement and shear at the pier top, but negligible moment. Shear and moment at the pier base also increase with the top mass. Lower foundation stiffness increases the pier top displacement, and reduces moment. On the other hand, it may increase or decrease the shear for the typical stiffness ratios studied here. The probabilistic spectrum of relative displacement between the bridge superstructure and the pier top much depends on the relative modal properties of the two systems.

ACKNOWLEDGEMENTS

Ms. Juan Peng, a graduate research assistant with Wayne State University, assisted in preparing the numerical examples. The Federal Highway Administration partially funded this work.

APPENDIX I

$R_{ff}(\tau)$ is the Fourier inverse transform of $S_{ff}(\omega)$

$$R_{ff}(\tau) = \int_{-\infty}^{\infty} S_{gg}(\omega) \exp(\mathrm{i}\omega\tau)\, \mathrm{d}\omega \tag{47}$$

$$R_{ff}(\tau) = \frac{S_0}{4} \sum_{k=1,2} \frac{1}{\zeta_{gk}\omega_{gk}} \exp(-\zeta_{gk}\omega_{gk}|\tau|)\left[(C_{ak} + C_{bk})\cos\omega_{gdk}|\tau| + \frac{\zeta_{gk}\omega_{gk}}{\omega_{gdk}}(C_{ak} - C_{bk})\sin\omega_{gdk}|\tau|\right] \tag{48}$$

where C_{ak} and C_{bk} (k = 1, 2) are:

$$C_{a1} = -\frac{\omega_{g1}^6}{D}\left[(1 + 8\zeta_{g1}^2 - 16\zeta_{g1}^4)\left(1 - \frac{\omega_{g1}^4}{\omega_{g2}^4}\right) - 8\zeta_{g1}^2\frac{\omega_{g1}^2}{\omega_{g2}^2}\left(1 - 2\zeta_{g2}^2 - \frac{\omega_{g1}^2}{\omega_{g2}^2} + 2\zeta_{g1}^2\frac{\omega_{g1}^2}{\omega_{g2}^2}\right)\right] \tag{49}$$

$$C_{b1} = \frac{2\omega_{g1}^6}{D}\left[(1 + 8\zeta_{g1}^2 - 16\zeta_{g1}^4)\left(1 - 2\zeta_{g1}^2 - \frac{\omega_{g1}^2}{\omega_{g2}^2} + 2\zeta_{g2}^2\frac{\omega_{g1}^2}{\omega_{g2}^2}\right) - 2\zeta_{g1}^2\left(1 - \frac{\omega_{g1}^4}{\omega_{g2}^4}\right)\right] \tag{50}$$

$$C_{a2} = \frac{\omega_{g1}^4\omega_{g2}^2}{D}\left[(1 + 8\zeta_{g1}^2 - 16\zeta_{g1}^4)\left(1 - \frac{\omega_{g1}^4}{\omega_{g2}^4}\right) - 8\zeta_{g1}^2\frac{\omega_{g1}^2}{\omega_{g2}^2}\left(1 - 2\zeta_{g2}^2 - \frac{\omega_{g1}^2}{\omega_{g2}^2} + 2\zeta_{g1}^2\frac{\omega_{g1}^2}{\omega_{g2}^2}\right)\right] \tag{51}$$

$$C_{b2} = \frac{2\omega_{g1}^2\omega_{g2}^4}{D}\left[\frac{\omega_{g1}^2}{\omega_{g2}^2}\left(-\frac{\omega_{g1}^2}{\omega_{g2}^2} - 8\zeta_{g1}^2 + 16\zeta_{g1}^2\zeta_{g2}^2\right)\left(1 - 2\zeta_{g1}^2 - \frac{\omega_{g1}^2}{\omega_{g2}^2} + 2\zeta_{g2}^2\frac{\omega_{g1}^2}{\omega_{g2}^2}\right) + 2\zeta_{g1}^2\left(1 - \frac{\omega_{g1}^4}{\omega_{g2}^4}\right)\right] \tag{52}$$

$$D = -4\omega_{g1}^2\omega_{g2}^2\left(1 - 2\zeta_{g1}^2 - \frac{\omega_{g1}^2}{\omega_{g2}^2} + 2\zeta_{g2}^2\frac{\omega_{g1}^2}{\omega_{g2}^2}\right)\left(1 - 2\,\zeta_{g2}^2 - \frac{\omega_{g1}^2}{\omega_{g2}^2} + 2\zeta_{g1}^2\frac{\omega_{g1}^2}{\omega_{g2}^2}\right) + \omega_{g2}^4\left(1 - \frac{\omega_{g1}^4}{\omega_{g2}^4}\right)^2 \tag{53}$$

APPENDIX II

$$\mathbf{B}_{mn}(t) = \begin{bmatrix} B_{mn,11} & B_{mn,12} & B_{mn,13} \\ B_{mn,21} & B_{mn,22} & B_{mn,23} \\ B_{mn,31} & B_{mn,32} & B_{mn,33} \end{bmatrix} \tag{54}$$

$$\begin{aligned} B_{mn,11}(t) &= S_0 \exp(-\omega_m\zeta_m - \omega_n\zeta_n)t \sum_{k=1,2} \frac{1}{16\zeta_{gk}\omega_{gk}} \sum_{i=1,N} \sum_{j=1,N} A_i A_j \\ &\times \{(C_{ak} + C_{bk})[g_1(\alpha_{km}, \alpha_{kn}, \rho_{jkm}, \mu_{ikn}) - g_2(\alpha_{km}, \beta_{kn}, \rho_{jkm}, \mu_{ikn}) + g_3(\alpha_{km}, \alpha_{kn}, \rho_{jkm}, \mu_{ikn}) - g_4(\alpha_{km}, \beta_{kn}, \rho_{jkm}, \mu_{ikn}) \\ &+ g_1(\beta_{km}, \beta_{kn}, \rho_{jkm}, \mu_{ikn}) - g_2(\beta_{km}, \alpha_{kn}, \rho_{jkm}, \mu_{ikn}) + g_3(\beta_{km}, \beta_{kn}, \rho_{jkm}, \mu_{ikn}) - g_4(\beta_{km}, \alpha_{kn}, \rho_{jkm}, \mu_{ikn}) \\ &+ g_5(\alpha_{km}, \alpha_{kn}, \mu_{jkm}, \rho_{ikn}) - g_6(\alpha_{km}, \beta_{kn}, \mu_{jkm}, \rho_{ikn}) + g_7(\alpha_{km}, \alpha_{kn}, \mu_{jkm}, \rho_{ikn}) - g_8(\alpha_{km}, \beta_{kn}, \mu_{jkm}, \rho_{ikn}) \\ &+ g_5(\beta_{km}, \beta_{kn}, \mu_{jkm}, \rho_{ikn}) - g_6(\beta_{km}, \alpha_{kn}, \mu_{jkm}, \rho_{ikn}) + g_7(\beta_{km}, \beta_{kn}, \mu_{jkm}, \rho_{ikn}) - g_8(\beta_{km}, \alpha_{kn}, \mu_{jkm}, \rho_{ikn}) \\ &+ \zeta_{gk}\omega_{gk}/\omega_{gdk}(C_{ak} - C_{bk})^* \\ &[g_9(\alpha_{km}, \alpha_{kn}, \rho_{jkm}, \mu_{ikn}) - g_{10}(\alpha_{km}, \beta_{kn}, \rho_{jkm}, \mu_{ikn}) + g_{11}(\alpha_{km}, \alpha_{kn}, \rho_{jkm}, \mu_{ikn}) - g_{12}(\alpha_{km}, \beta_{kn}, \rho_{jkm}, \mu_{ikn}) \\ &- g_9(\beta_{km}, \beta_{kn}, \rho_{jkm}, \mu_{ikn}) + g_{10}(\beta_{km}, \alpha_{kn}, \rho_{jkm}, \mu_{ikn}) - g_{11}(\beta_{km}, \beta_{kn}, \rho_{jkm}, \mu_{ikn}) + g_{12}(\beta_{km}, \alpha_{kn}, \rho_{jkm}, \mu_{ikn}) \\ &+ g_{13}(\alpha_{km}, \alpha_{kn}, \mu_{jkm}, \rho_{ikn}) - g_{14}(\alpha_{km}, \beta_{kn}, \mu_{jkm}, \rho_{ikn}) + g_{15}(\alpha_{km}, \alpha_{kn}, \mu_{jkm}, \rho_{ikn}) - g_{16}(\alpha_{km}, \beta_{kn}, \mu_{jkm}, \rho_{ikn}) \\ &- g_{13}(\beta_{km}, \beta_{kn}, \mu_{jkm}, \rho_{ikn}) + g_{14}(\beta_{km}, \alpha_{kn}, \mu_{jkm}, \rho_{ikn}) - g_{15}(\beta_{km}, \beta_{kn}, \mu_{jkm}, \rho_{ikn}) + g_{16}(\beta_{km}, \alpha_{kn}, \mu_{jkm}, \rho_{ikn})]\} \end{aligned} \tag{55}$$

$$B_{mn,12}(t) = B_{nm,21}(t) \tag{56}$$

$$\begin{aligned} B_{mn,13}(t) &= S_0 \left[\sum_{i=1,N} A_i \exp(B_i t)\right] \sum_{k=1,2} \frac{1}{8\zeta_{gk}\omega_{gk}} \sum_{j=1,N} A_j \exp(B_j t) \\ &\times \{(C_{ak} + C_{bk})[g_{18}(\alpha_{km}, \rho_{jkm}) + g_{18}(\beta_{km}, \rho_{jkm})] \\ &+ \zeta_{gk}\omega_{gk}/\omega_{gdk}(C_{ak} - C_{bk})[-g_{17}(\alpha_{km}, \rho_{jkm}) + g_{17}(\beta_{km}, \rho_{jkm})]\} \end{aligned} \tag{57}$$

$$\begin{aligned} B_{mn,21}(t) &= S_0 \exp(-\omega_m\zeta_m - \omega_n\zeta_n)t \sum_{k=1,2} \frac{1}{16\zeta_{gk}\omega_{gk}} \sum_{i=1,N} \sum_{j=1,N} A_i A_j \\ &\times \{(C_{ak} + C_{bk})[-g_9(\alpha_{km}, \alpha_{kn}, \rho_{jkm}, \mu_{ikn}) + g_{10}(\alpha_{km}, \beta_{kn}, \rho_{jkm}, \mu_{ikn}) - g_{11}(\alpha_{km}, \alpha_{kn}, \rho_{jkm}, \mu_{ikn}) \\ &+ g_{12}(\alpha_{km}, \beta_{kn}, \rho_{jkm}, \mu_{ikn}) - g_9(\beta_{km}, \beta_{kn}, \rho_{jkm}, \mu_{ikn}) + g_{10}(\beta_{km}, \alpha_{kn}, \rho_{jkm}, \mu_{ikn}) - g_{11}(\beta_{km}, \beta_{kn}, \rho_{jkm}, \mu_{ikn}) \\ &+ g_{12}(\beta_{km}, \alpha_{kn}, \rho_{jkm}, \mu_{ikn}) + g_{13}(\alpha_{km}, \alpha_{kn}, \mu_{jkm}, \rho_{ikn}) - g_{14}(\alpha_{km}, \beta_{kn}, \mu_{jkm}, \rho_{ikn}) + g_{15}(\alpha_{km}, \alpha_{kn}, \mu_{jkm}, \rho_{ikn}) \\ &- g_{16}(\alpha_{km}, \beta_{kn}, \mu_{jkm}, \rho_{ikn}) + g_{13}(\beta_{km}, \beta_{kn}, \mu_{jkm}, \rho_{ikn}) - g_{14}(\beta_{km}, \alpha_{kn}, \mu_{jkm}, \rho_{ikn}) + g_{15}(\beta_{km}, \beta_{kn}, \mu_{jkm}, \rho_{ikn}) \\ &- g_{16}(\beta_{km}, \alpha_{kn}, \mu_{jkm}, \rho_{ikn}) + \zeta_{gk}\omega_{gk}/\omega_{gdk}(C_{ak} - C_{bk}) \\ &\times [g_1(\alpha_{km}, \alpha_{kn}, \rho_{jkm}, \mu_{ikn}) - g_2(\alpha_{km}, \beta_{kn}, \rho_{jkm}, \mu_{ikn}) + g_3(\alpha_{km}, \alpha_{kn}, \rho_{jkm}, \mu_{ikn}) - g_4(\alpha_{km}, \beta_{kn}, \rho_{jkm}, \mu_{ikn}) \\ &- g_1(\beta_{km}, \beta_{kn}, \rho_{jkm}, \mu_{ikn}) + g_2(\beta_{km}, \alpha_{kn}, \rho_{jkm}, \mu_{ikn}) - g_3(\beta_{km}, \beta_{kn}, \rho_{jkm}, \mu_{ikn}) + g_4(\beta_{km}, \alpha_{kn}, \rho_{jkm}, \mu_{ikn}) \\ &- g_5(\alpha_{km}, \alpha_{kn}, \mu_{jkm}, \rho_{ikn}) + g_6(\alpha_{km}, \beta_{kn}, \mu_{jkm}, \rho_{ikn}) - g_7(\alpha_{km}, \alpha_{kn}, \mu_{jkm}, \rho_{ikn}) + g_8(\alpha_{km}, \beta_{kn}, \mu_{jkm}, \rho_{ikn}) \\ &+ g_5(\beta_{km}, \beta_{kn}, \mu_{jkm}, \rho_{ikn}) - g_6(\beta_{km}, \alpha_{kn}, \mu_{jkm}, \rho_{ikn}) + g_7(\beta_{km}, \beta_{kn}, \mu_{jkm}, \rho_{ikn}) - g_8(\beta_{km}, \alpha_{kn}, \mu_{jkm}, \rho_{ikn})]\} \end{aligned} \tag{58}$$

$$B_{mn,22}(t) = S_0 \exp(-\omega_m\zeta_m - \omega_n\zeta_n)t \sum_{k=1,2} \frac{1}{16\zeta_{gk}\omega_{gk}} \sum_{i=1,N} \sum_{j=1,N} A_i A_j$$
$$\times \{(C_{ak} + C_{bk})[g_1(\alpha_{km}, \alpha_{kn}, \rho_{jkm}, \mu_{ikn}) + g_2(\alpha_{km}, \beta_{kn}, \rho_{jkm}, \mu_{ikn}) + g_3(\alpha_{km}, \alpha_{kn}, \rho_{jkm}, \mu_{ikn})$$
$$+ g_4(\alpha_{km}, \beta_{kn}, \rho_{jkm}, \mu_{ikn}) + g_1(\beta_{km}, \beta_{kn}, \rho_{jkm}, \mu_{ikn}) + g_2(\beta_{km}, \alpha_{kn}, \rho_{jkm}, \mu_{ikn}) + g_3(\beta_{km}, \beta_{kn}, \rho_{jkm}, \mu_{ikn})$$
$$+ g_4(\beta_{km}, \alpha_{kn}, \rho_{jkm}, \mu_{ikn}) + g_5(\alpha_{km}, \alpha_{kn}, \mu_{jkm}, \rho_{ikn}) + g_6(\alpha_{km}, \beta_{kn}, \mu_{jkm}, \rho_{ikn}) + g_7(\alpha_{km}, \alpha_{kn}, \mu_{jkm}, \rho_{ikn})$$
$$+ g_8(\alpha_{km}, \beta_{kn}, \mu_{jkm}, \rho_{ikn}) + g_5(\beta_{km}, \beta_{kn}, \mu_{jkm}, \rho_{ikn}) + g_6(\beta_{km}, \alpha_{kn}, \mu_{jkm}, \rho_{ikn}) + g_7(\beta_{km}, \beta_{kn}, \mu_{jkm}, \rho_{ikn})$$
$$+ g_8(\beta_{km}, \alpha_{kn}, \mu_{jkm}, \rho_{ikn})] + \zeta_{gk}\omega_{gk}/\omega_{gdk}(C_{ak} - C_{bk})$$
$$\times [g_9(\alpha_{km}, \alpha_{kn}, \rho_{jkm}, \mu_{ikn}) + g_{10}(\alpha_{km}, \beta_{kn}, \rho_{jkm}, \mu_{ikn}) + g_{11}(\alpha_{km}, \alpha_{kn}, \rho_{jkm}, \mu_{ikn}) + g_{12}(\alpha_{km}, \beta_{kn}, \rho_{jkm}, \mu_{ikn})$$
$$- g_9(\beta_{km}, \beta_{kn}, \rho_{jkm}, \mu_{ikn}) - g_{10}(\beta_{km}, \alpha_{kn}, \rho_{jkm}, \mu_{ikn}) - g_{11}(\beta_{km}, \beta_{kn}, \rho_{jkm}, \mu_{ikn}) - g_{12}(\beta_{km}, \alpha_{kn}, \rho_{jkm}, \mu_{ikn})$$
$$+ g_{13}(\alpha_{km}, \alpha_{kn}, \mu_{jkm}, \rho_{ikn}) + g_{14}(\alpha_{km}, \beta_{kn}, \mu_{jkm}, \rho_{ikn}) + g_{15}(\alpha_{km}, \alpha_{kn}, \mu_{jkm}, \rho_{ikn}) + g_{16}(\alpha_{km}, \beta_{kn}, \mu_{jkm}, \rho_{ikn})$$
$$- g_{13}(\beta_{km}, \beta_{kn}, \mu_{jkm}, \rho_{ikn}) - g_{14}(\beta_{km}, \alpha_{kn}, \mu_{jkm}, \rho_{ikn}) - g_{15}(\beta_{km}, \beta_{kn}, \mu_{jkm}, \rho_{ikn}) - g_{16}(\beta_{km}, \alpha_{kn}, \mu_{jkm}, \rho_{ikn})]\} \quad (59)$$

$$B_{mn,23}(t) = S_0 \left[\sum_{i=1,N} A_i \exp(B_i t)\right] \sum_{k=1,2} \frac{1}{8\zeta_{gk}\omega_{gk}} \sum_{j=1,N} A_j \exp(B_j t)$$
$$\times \{(C_{ak} + C_{bk})[g_{17}(\alpha_{km}, \rho_{jkm}) + g_{17}(\beta_{km}, \rho_{jkm})] + \zeta_{gk}\omega_{gk}/\omega_{gdk}(C_{ak} - C_{bk})[g_{18}(\alpha_{km}, \rho_{jk}) - g_{18}(\beta_{km}, \rho_{jkm})]\} \quad (60)$$

$$B_{mn,31}(t) = B_{nm,13}(t) \quad (61)$$

$$B_{mn,32}(t) = B_{nm,23}(t) \quad (62)$$

$$B_{mn,33}(t) = \left[\sum_{i=1,N} A_i \exp(B_i t)\right]^2 R_{gg}(0) \quad (63)$$

where functions g_1 through g_{18} are given as follows:

$$g_1(\alpha_{km}, \alpha_{kn}, \rho_{jkm}, \mu_{ikn}) = \{[-\rho_{jkm}\cos(\alpha_{km} - \alpha_{kn})t + \alpha_{km}\sin(\alpha_{km} - \alpha_{kn})t][\exp(\mu_{ikn}t)(\alpha_{kn}\sin\alpha_{kn}t$$
$$+ \mu_{ikn}\cos\alpha_{kn}t) - \mu_{ikn}] + [\alpha_{km}\cos(\alpha_{km} - \alpha_{kn})t + \rho_{jkm}\sin(\alpha_{km} - \alpha_{kn})t]$$
$$\times [\exp(\mu_{ikn}t)(\mu_{ikn}\sin\alpha_{kn}t - \alpha_{kn}\cos\alpha_{kn}t) + \alpha_{kn}]\}/[(\rho_{jkm}^2 + \alpha_{km}^2)(\mu_{ikn}^2 + \alpha_{kn}^2)] \quad (64)$$

$$g_2(\alpha_{km}, \beta_{kn}, \rho_{jkm}, \mu_{ikn}) = \{[\rho_{jkm}\cos(\alpha_{km} + \beta_{kn})t - \alpha_{km}\sin(\alpha_{km} + \beta_{kn})t][\exp(\mu_{ikn}t)(\beta_{kn}\sin\beta_{kn}t$$
$$+ \mu_{ikn}\cos\beta_{kn}t) - \mu_{ikn}] + [\alpha_{km}\cos(\alpha_{km} + \beta_{kn})t + \rho_{jkm}\sin(\alpha_{km} + \beta_{kn})t]$$
$$\times [\exp(\mu_{ikn}t)(\mu_{ikn}\sin\beta_{kn}t - \beta_{kn}\cos\beta_{kn}t) + \beta_{kn}]\}/[(\rho_{jkm}^2 + \alpha_{km}^2)(\mu_{ikn}^2 + \beta_{kn}^2)] \quad (65)$$

$$g_3(\alpha_{km}, \alpha_{kn}, \rho_{jkm}, \mu_{ikn}) = \{[\rho_{jkm}\cos(\alpha_{km} - \alpha_{kn})t - \alpha_{km}\sin(\alpha_{km} - \alpha_{kn})t]$$
$$\times [\exp(\rho_{jkm} + \mu_{ikn})t((\alpha_{km} - \alpha_{kn})\sin(\alpha_{km} - \alpha_{kn})t + (\rho_{jkm} + \mu_{ikn})\cos(\alpha_{km} - \alpha_{kn})t) - (\rho_{jkm} + \mu_{ikn})]$$
$$+ [\alpha_{km}\cos(\alpha_{km} - \alpha_{kn})t + \rho_{jkm}\sin(\alpha_{km} - \alpha_{kn})t]$$
$$\times [\exp(\rho_{jkm} + \mu_{ikn})t((\rho_{jkm} + \mu_{ikn})\sin(\alpha_{km} - \alpha_{kn})t - (\alpha_{km} - \alpha_{kn})\cos(\alpha_{km} - \alpha_{kn})t) + (\alpha_{km} - \alpha_{kn})]\}$$
$$/\{(\rho_{jkm}^2 + \alpha_{km}^2)[(\rho_{jkm} + \mu_{ikn})^2 + (\alpha_{km} - \alpha_{kn})^2]\} \quad (66)$$

$$g_4(\alpha_{km}, \beta_{kn}, \rho_{jkm}, \mu_{ikn}) = \{[-\rho_{jkm}\cos(\alpha_{km} + \beta_{kn})t + \alpha_{km}\sin(\alpha_{km} + \beta_{kn})t]$$
$$\times [\exp(\rho_{jkm} + \mu_{ikn})t((\alpha_{km} + \beta_{kn})\sin(\alpha_{km} + \beta_{kn})t + (\rho_{jkm} + \mu_{ikn})\cos(\alpha_{km} + \beta_{kn})t) - (\rho_{jkm} + \mu_{ikn})]$$
$$- [\rho_{jkm}\sin(\alpha_{km} + \beta_{kn})t + \alpha_{km}\cos(\alpha_{km} + \beta_{kn})t]$$
$$\times [\exp(\rho_{jkm} + \mu_{ikn})t((\rho_{jkm} + \mu_{ikn})\sin(\alpha_{km} + \beta_{kn})t - (\alpha_{km} + \beta_{kn})\cos(\alpha_{km} + \beta_{kn})t) + (\alpha_{km} + \beta_{kn})]\}$$
$$/\{(\rho_{jkm}^2 + \alpha_{km}^2)[(\rho_{jkm} + \mu_{ikn})^2 + (\alpha_{km} + \beta_{kn})^2]\} \quad (67)$$

$$g_5(\alpha_{km}, \alpha_{kn}, \mu_{jkm}, \rho_{ikn}) = \exp(\mu_{jkm}t)\{(\mu_{jkm}\cos\alpha_{kn}t + \alpha_{km}\sin\alpha_{kn}t)[\exp(\rho_{ikn}t)(\alpha_{kn}\sin\alpha_{kn}t + \rho_{ikn}\cos\alpha_{kn}t) - \rho_{ikn}]$$
$$+ (\alpha_{km}\cos\alpha_{kn}t - \mu_{jkm}\sin\alpha_{kn}t)[\exp(\rho_{ikn}t)(-\rho_{ikn}\sin\alpha_{kn}t + \alpha_{kn}\cos\alpha_{kn}t) - \alpha_{kn}]\}$$
$$/[(\mu_{jkm}^2 + \alpha_{km}^2)(\rho_{ikn}^2 + \alpha_{kn}^2)] \tag{68}$$

$$g_6(\alpha_{km}, \beta_{kn}, \mu_{jkm}, \rho_{ikn}) = \exp(\mu_{jkm}t)\{(-\mu_{jkm}\cos\beta_{kn}t + \alpha_{km}\sin\beta_{kn}t)[\exp(\rho_{ikn}t)(\beta_{kn}\sin\beta_{kn}t + \rho_{ikn}\cos\beta_{kn}t) - \rho_{ikn}]$$
$$- (\alpha_{km}\cos\beta_{kn}t + \mu_{jkm}\sin\beta_{kn}t)[\exp(\rho_{ikn}t)(\rho_{ikn}\sin\beta_{kn}t - \beta_{kn}\cos\beta_{kn}t) + \beta_{kn}]\}$$
$$/[(\mu_{jkm}^2 + \alpha_{km}^2)(\rho_{ikn}^2 + \beta_{kn}^2)] \tag{69}$$

$$g_7(\alpha_{km}, \alpha_{kn}, \mu_{jkm}, \rho_{ikn}) = \{[-\mu_{jkm}\cos(\alpha_{km} - \alpha_{kn})t + \alpha_{km}\sin(\alpha_{km} - \alpha_{kn})t]$$
$$\times [\exp(\mu_{jkm} + \rho_{ikn})t((\alpha_{km} - \alpha_{kn})\sin(\alpha_{km} - \alpha_{kn})t + (\mu_{jkm} + \rho_{ikn})\cos(\alpha_{km} - \alpha_{kn})t) - (\mu_{jkm} + \rho_{ikn})]$$
$$- [\alpha_{km}\cos(\alpha_{km} - \alpha_{kn})t + \mu_{jkm}\sin(\alpha_{km} - \alpha_{kn})t]$$
$$\times [\exp(\mu_{jkm} + \rho_{jkn})t((\mu_{jkm} + \rho_{ikn})\sin(\alpha_{km} - \alpha_{kn})t - (\alpha_{km} - \alpha_{kn})\cos(\alpha_{km} - \alpha_{kn})t) + (\alpha_{km} - \alpha_{kn})]\}$$
$$/\{(\mu_{jkm}^2 + \alpha_{km}^2)[(\mu_{jkm} + \rho_{ikn})^2 + (\alpha_{km} - \alpha_{kn})^2]\} \tag{70}$$

$$g_8(\alpha_{km}, \beta_{kn}, \mu_{jkm}, \rho_{ikn}) = \{[\mu_{jkm}\cos(\alpha_{km} + \beta_{kn})t - \alpha_{km}\sin(\alpha_{km} + \beta_{kn})t]$$
$$\times [\exp(\mu_{jkm} + \rho_{ikn})t((\alpha_{km} + \beta_{kn})\sin(\alpha_{km} + \beta_{kn})t + (\mu_{jkm} + \rho_{ikn})\cos(\alpha_{km} + \beta_{kn})t) - (\mu_{jkm} + \rho_{ikn})]$$
$$+ [\alpha_{km}\cos(\alpha_{km} + \beta_{kn})t + \mu_{jkm}\sin(\alpha_{km} + \beta_{kn})t]$$
$$\times [\exp(\mu_{jkm} + \rho_{ikn})t((\mu_{jkm} + \rho_{ikn})\sin(\alpha_{km} + \beta_{kn})t - (\alpha_{km} + \beta_{kn})\cos(\alpha_{km} + \beta_{kn})t) + (\alpha_{km} + \beta_{kn})]\}$$
$$/\{(\mu_{jkm}^2 + \alpha_{km}^2)[(\mu_{jkm} + \rho_{ikn})^2 + (\alpha_{km} + \beta_{kn})^2]\} \tag{71}$$

$$g_9(\alpha_{km}, \alpha_{kn}, \rho_{jkm}, \mu_{ikn}) = \{[\alpha_{km}\cos(\alpha_{km} - \alpha_{kn})t + \rho_{jkm}\sin(\alpha_{km} - \alpha_{kn})t][\exp(\mu_{ikn}t)(\alpha_{kn}\sin\alpha_{kn}t + \mu_{ikn}\cos\alpha_{kn}t) - \mu_{ikn}]$$
$$+ [\rho_{jkm}\cos(\alpha_{km} - \alpha_{kn})t - \alpha_{km}\sin(\alpha_{km} - \alpha_{kn})t][\exp(\mu_{ikn}t)(\mu_{ikn}\sin\alpha_{kn}t - \alpha_{kn}\cos\alpha_{kn}t) + \alpha_{kn}]\}$$
$$/[(\rho_{jkm}^2 + \alpha_{km}^2)(\mu_{ikn}^2 + \alpha_{kn}^2)] \tag{72}$$

$$g_{10}(\alpha_{km}, \beta_{kn}, \rho_{jkm}, \mu_{ikn}) = \{[-\rho_{jkm}\sin(\alpha_{km} + \beta_{kn})t - \alpha_{km}\cos(\alpha_{km} + \beta_{kn})t][\exp(\mu_{ikn}t)(\beta_{kn}\sin\beta_{kn}t$$
$$+ \mu_{ikn}\cos\beta_{kn}t) - \mu_{ikn}] + [\rho_{jkm}\cos(\alpha_{km} + \beta_{kn})t - \alpha_{km}\sin(\alpha_{km} + \beta_{kn})t][\exp(\mu_{ikn}t)(\mu_{ikn}\sin\beta_{kn}t$$
$$- \beta_{kn}\cos\beta_{kn}t) + \beta_{kn}]\}/[(\rho_{jkm}^2 + \alpha_{km}^2)(\mu_{ikn}^2 + \beta_{kn}^2)] \tag{73}$$

$$g_{11}(\alpha_{km}, \alpha_{kn}, \rho_{jkm}, \mu_{ikn}) = \{[-\rho_{jkm}\sin(\alpha_{km} - \alpha_{kn})t - \alpha_{km}\cos(\alpha_{km} - \alpha_{kn})t]$$
$$\times [\exp(\rho_{jkm} + \mu_{ikn})t((\alpha_{km} - \alpha_{kn})\sin(\alpha_{km} - \alpha_{kn})t + (\rho_{jkm} + \mu_{ikn})\cos(\alpha_{km} - \alpha_{kn})t - (\rho_{jkm} + \mu_{ikn})]$$
$$+ [-\alpha_{km}\sin(\alpha_{km} - \alpha_{kn})t + \rho_{jkm}\cos(\alpha_{km} - \alpha_{kn})t]$$
$$\times [\exp(\rho_{jkm} + \mu_{ikn})t((\rho_{jkm} + \mu_{ikn})\sin(\alpha_{km} - \alpha_{kn})t - (\alpha_{km} - \alpha_{kn})\cos(\alpha_{km} - \alpha_{kn})t) + (\alpha_{km} - \alpha_{kn})]\}$$
$$/\{(\rho_{jkm}^2 + \alpha_{km}^2)[(\rho_{jkm} + \mu_{ikn})^2 + (\alpha_{km} - \alpha_{kn})^2]\} \tag{74}$$

$$g_{12}(\alpha_{km}, \beta_{kn}, \rho_{jkm}, \mu_{ikn}) = \{[\rho_{jkm}\sin(\alpha_{km} + \alpha_{kn})t + \alpha_{km}\cos(\alpha_{km} + \alpha_{kn})t]$$
$$\times [\exp(\rho_{jkm} + \mu_{ikn})t((\alpha_{km} + \alpha_{kn})\sin(\alpha_{km} + \alpha_{kn})t + (\rho_{jkm} + \mu_{ikn})\cos(\alpha_{km} + \alpha_{kn})t) - (\rho_{jkm} + \mu_{ikn})]$$
$$+ [\alpha_{km}\sin(\alpha_{km} + \alpha_{kn})t - \rho_{jkm}\cos(\alpha_{km} + \alpha_{kn})t]$$
$$\times [\exp(\rho_{jkm} + \mu_{ikn})t((\rho_{jkm} + \mu_{ikn})\sin(\alpha_{km} + \alpha_{kn})t - (\alpha_{km} + \alpha_{kn})\cos(\alpha_{km} + \alpha_{kn})t) + (\alpha_{km} + \alpha_{kn})]\}$$
$$/\{(\rho_{jkm}^2 + \alpha_{km}^2)[(\rho_{jkm} + \mu_{ikn})^2 + (\alpha_{km} + \alpha_{kn})^2]\} \tag{75}$$

$$g_{13}(\alpha_{km},\alpha_{kn},\mu_{jkm},\rho_{ikn}) = -\exp(\mu_{jkm}t)\{(-\alpha_{km}\cos\alpha_{kn}t+\mu_{jkm}\sin\alpha_{kn}t)[\exp(\rho_{ikn}t)(\alpha_{kn}\sin\alpha_{kn}t+\rho_{ikn}\cos\alpha_{kn}t)-\rho_{ikn}]$$
$$+\mu_{jkm}\cos\alpha_{kn}t+\alpha_{km}\sin\alpha_{kn}t)[\exp(\rho_{ikn}t)(-\rho_{ikn}\sin\alpha_{kn}t+\alpha_{kn}\cos\alpha_{kn}t)-\alpha_{kn}]\}$$
$$/[(\mu_{jkm}^2+\alpha_{km}^2)(\rho_{ikn}^2+\alpha_{kn}^2)] \tag{76}$$

$$g_{14}(\alpha_{km},\beta_{kn},\mu_{jkm},\rho_{ikn}) = -\exp(\mu_{jkm}t)\{(\alpha_{km}\cos\beta_{kn}t+\mu_{jkm}\sin\beta_{kn}t)[\exp(\rho_{ikn}t)(\beta_{kn}\sin\beta_{kn}t+\rho_{ikn}\cos\beta_{kn}t)-\rho_{ikn}]$$
$$-(\mu_{jkm}\cos\beta_{kn}t-\alpha_{km}\sin\beta_{kn}t)[\exp(\rho_{ikn}t)(\rho_{ikn}\sin\beta_{kn}t-\beta_{kn}\cos\beta_{kn}t)+\beta_{kn}]\}$$
$$/[(\mu_{jkm}^2+\alpha_{km}^2)(\rho_{ikn}^2+\beta_{kn}^2)] \tag{77}$$

$$g_{15}(\alpha_{km},\alpha_{kn},\mu_{jkm},\rho_{ikn}) = \{-[\mu_{jkm}\sin(\alpha_{km}-\alpha_{kn})t+\alpha_{km}\cos(\alpha_{km}-\alpha_{kn})t]$$
$$\times[\exp(\mu_{jkm}+\rho_{ikn})t[(\alpha_{km}-\alpha_{kn})\sin(\alpha_{km}-\alpha_{kn})t+(\mu_{jkm}+\rho_{ikn})\cos(\alpha_{km}-\alpha_{kn})t]-(\mu_{jkm}+\rho_{ikn})]$$
$$+[-\alpha_{km}\sin(\alpha_{km}-\alpha_{kn})t+\rho_{jkm}\cos(\alpha_{km}-\alpha_{kn})t]$$
$$\times[\exp(\rho_{jkm}+\mu_{ikn})t[(\rho_{jkm}+\mu_{ikn})\sin(\alpha_{km}-\alpha_{kn})t-(\alpha_{km}-\alpha_{kn})\cos(\alpha_{km}-\alpha_{kn})t]+(\alpha_{km}-\alpha_{kn})]\}$$
$$/\{(\mu_{jkm}^2+\alpha_{km}^2)[(\mu_{jkm}+\rho_{ikn})^2+(\alpha_{km}-\alpha_{kn})^2]\} \tag{78}$$

$$g_{16}(\alpha_{km},\beta_{kn},\mu_{jkm},\rho_{ikn}) = \{[\mu_{jkm}\sin(\alpha_{km}+\beta_{kn})t+\alpha_{km}\cos(\alpha_{km}+\beta_{kn})t]$$
$$\times[\exp(\mu_{jkm}+\rho_{ikn})t[(\alpha_{km}+\beta_{kn})\sin(\alpha_{km}+\beta_{kn})t+(\mu_{jkm}+\rho_{ikn})\cos(\alpha_{km}+\beta_{kn})t]-(\mu_{jkm}+\rho_{ikn})]$$
$$+[\alpha_{km}\sin(\alpha_{km}+\beta_{kn})t-\mu_{jkm}\cos(\alpha_{km}+\beta_{kn})t]$$
$$\times[\exp(\mu_{jkm}+\rho_{ikn})t[(\mu_{jkm}+\rho_{ikn})\sin(\alpha_{km}+\beta_{kn})t-(\alpha_{km}+\beta_{kn})\cos(\alpha_{km}+\beta_{kn})t]+(\alpha_{km}+\beta_{kn})]\}$$
$$/\{(\mu_{jkm}^2+\alpha_{km}^2)[(\mu_{jkm}+\rho_{ikn})^2+(\alpha_{km}+\beta_{kn})^2]\} \tag{79}$$

$$f_{17}(\alpha_{km},\rho_{jkm}) = [\exp(-\rho_{jkm}t)(-\rho_{jkm}\sin\alpha_{km}t-\alpha_{km}\cos\alpha_{km}t)+\alpha_{km}]/(\rho_{jkm}^2+\alpha_{km}^2) \tag{80}$$

$$f_{18}(\alpha_{km},\rho_{jkm}) = [\exp(-\rho_{jkm}t)(\alpha_{km}\sin\alpha_{km}t-\rho_{jkm}\cos\alpha_{km}t)+\rho_{jkm}]/(\rho_{jkm}^2+\alpha_{km}^2) \tag{81}$$

where α_{km}, β_{kn}, μ_{jkm}, and ρ_{ikn} are functions of the system parameters given below:

$$\alpha_{km}=\omega_{dm}-\omega_{gdk},\ \beta_{kn}=\omega_{dn}+\omega_{gdk},\ \rho_{jkm}=B_j+\zeta_m\omega_m+\zeta_{gk}\omega_{gk},\ \mu_{ikn}=B_i+\zeta_n\omega_n-\zeta_{gk}\omega_{gk}$$
$$(i,j=1,2,\ldots,N;\ k=1,2;\ m,n=1,2,\ldots). \tag{82}$$

REFERENCES

1. A. Astaneh-Asl, B. Bolt, K. M. McMullin, R. R. Donikian, D. Modjtahedi, and S.-W. Cho, 'Seismic performance of steel bridges during the 1994 Northridge Earthquake', *Report to Caltrans*, *UCB/CE-Steel-94/01*, Dept. of Civil Engineering, UC Berkeley, April 1994.
2. C. D. Comartin, M. Greene and S. K. Tubbesing (eds), 'The Hyogo-Ken Nanbu earthquake, Jan. 17, 1995', *Preliminary Reconnaissance Report*, *EERI*, 1995.
3. R. W. Clough and J. Penzien. *Dynamics of Structures*, McGraw – Hill, New York, 1975.
4. C. G. Bucher, 'Approximate nonstationary random vibration analysis for MDOF systems', *J. App. Mech.* **55**, 197, 1988.
5. T. K. Caughey and H. F. Stumpf, 'Transit response of a dynamic system under random excitation', *J. Appl. Mech. ASME* **28**, 563, 1961.
6. R. B. Corotis and T. A. Marshall, 'Oscillator response to modulated random excitation', *ASCE J. Engng. Mech.* **103** (EM4), 501, 1977.
7. G. Fu, 'Seismic response statistics of SDOF system to exponentially modulated colored input: an explicit solution', *Earthquake Engng. Struct. Dyn.* **24**, (1995) (in press).
8. G. Fu and J. Lall, 'Modal analysis for cantilever beam response to nonstationary colored random excitation', in (ed.) S. Sture *Engng. Mechanics*, *Proc. ASCE 10th Engineering Mechanic Conf.*, Boulder, CO, 21–24, May 1995, p. 942.
9. D. A. Gasparini, 'Response of MDOF systems to nonstationary random excitation', *ASCE J. Engng Mech.* **105**, 13 (1979).
10. D. A. Gasparini and A. DebChaudhury, 'Dynamic response to nonstationary nonwhite excitation', *ASCE J. Engng. Mech.* **106**, 1233 (1980).

11. Z. K. Hou, 'Nonstationary response of structures and its application to earthquake engineering', *California Institute of Technology, EERL 90-01*, 1990.
12. W. D. Iwan and Z. K. Hou, 'Explicit solution for the response of simple systems subjected to nonstationary random excitation', *Struct. Safety* **6**, 77 (1989).
13. M. Shinozuka and Y. Sato, 'Simulation of nonstationary random process', *ASCE J. Engng. Mech. Div.* **93**, 11 (1967).
14. C.-H. Yeh and Y. K. Wen, 'Modeling of nonstationary ground motion and analysis of inelastic structural response, *Struct. Safety* **8**, 281 (1990)
15. Y. K. Lin, *Probabilistic Theory of Structural Dynamics*, R. E. Krieger Publishing Company, New York, 1967.

